

ATMOSPHERIC CHARACTERIZATION OF JUPITER USING A PLANETARY RADIATION TRANSPORT MODEL BASED ON MODTRAN^{®5}

Marsha J. Fox, Alexander Berk and Lawrence S. Bernstein

Spectral Sciences, Inc., Burlington, MA

ABSTRACT

We continue to upgrade our planetary radiation transfer (RT) model based on MODTRAN^{®5} to spectrally characterize the RT of planetary atmospheres. A key objective of our project is to develop a code that can be used by astronomers and planetary scientists in the search for planets in other star systems, or ‘exoplanets’. Already 373 gas giants have been detected orbiting 215 stars, but no terrestrial planets have been identified. Previously, we described modifications to MODTRAN^{®5} to make it more generally applicable to arbitrary atmospheres, showing comparisons to data and results of RT models developed by planetary scientists for gas giants Neptune and Saturn, over the full optical spectrum from UV through far-infrared spectral regime, ~0.4 to 200 μm . This year we model Jupiter, another gas giant that is well known for its diversity of atmospheric conditions – with large-scale temporal variability lasting 10s to 100s of years, including large bands of clouds, immense turbulent eddy plumes and dark ‘hot spot’ regions that light up in thermal bands. These regions are represented by varying levels of clouds, haze and absorption features. Clear-sky and multi-layer cloud models were developed for comparisons to observations of different spatial regions. Spectrally resolved observations from the Gemini’s Near-Infrared Mapping Spectrometer (NIMS) and Cassini’s Composite Infrared Spectrometer (CIRS) missions to Jupiter as well as observations from ground based systems have been used for comparison. .

1.0 INTRODUCTION

The rapid pace of exoplanet discovery (~357 to date) [1], underscores the need for fast and accessible spectral simulation and analysis codes. One of the primary science objectives of the upcoming James Webb Space Telescope mission [2], as well as similar planned missions by a number of other countries, is exoplanet discovery via spectroscopic observations. One of the planned detection techniques is transit spectroscopy [3],[4]. For this approach, very small modulations, typically of order 10^{-4} , of the total stellar emission, due to attenuation of the small fraction of light that passes through the planet’s atmosphere, are detected. The resulting modulation spectrum can be analyzed to determine the composition of the planetary atmosphere. A related approach, involves retrieval of the total planetary thermal emission spectrum by differencing the spectra obtained for the planet in front of and behind its parent star. For both of these methods, a generalized, well validated radiation transport model applicable to a wide variety of possible planetary atmospheres will be needed for comparison to measurements.

We have developed a generalized planetary radiation transfer (RT) model that is derived from MODTRAN^{®5} and uses all of its code structure and capabilities. MODTRAN^{®5} is the newest version of MODTRAN[®] and features 0.1 wavenumber spectral resolution for radiation transfer calculations between 0.4 and 10^4 micron wavelengths, and an enhanced capability to easily incorporate spectral band models for many new species [5]. The planetary RT code includes MODTRAN^{®5} band model databases extended to much lower temperatures (down to 30K).. Earlier modifications made to MODTRAN^{®5} to create the planetary RT model are described in references [6] and [7]. For this effort, a preliminary set of temperature-dependent shortwave NH_3 absorption coefficients, derived from the work of Bowles et al. [8], have been incorporated into our planetary RT model. The comparisons presented here to data and other RT models provide a source of validation for these new features of our planetary RT model.

Jupiter is well known for a varied atmosphere that includes hurricane-like features such as the Great Red Spot, greater in size than Earth’s diameter, and bands of varying shades, termed zones (light) and belts (dark) that are generally identified as regions of differing cloud opacity and characteristics. Although these are dynamic features, with localized plume structure that can change color frequently, the life span for most resolvable features is typically months to years. The overall band structure has been consistent over the past 30 years, as shown in Fig. 1 comparing the Hubble Space Telescope imagery from 1979 and 2000. Therefore, many of the measurements made from Voyager in 1979 missions are still considered a useful source of general planetary features. Thermal imagery of Jupiter taken by NASA’s Infrared Telescope Facility (IRTF) on Mauna Kea HI, during the Galileo mission in July, 1995 show that the belts have a significantly stronger thermal signature at 4.85 microns than zones, indicating

lower cloud opacity in this wavelength band that allows radiation observation down to lower and warmer levels within the atmosphere.



Fig. 1. Variation in Atmospheric Structure of Jupiter; Hubble Space Telescope Imagery of Jupiter from 1979 (left) and 2000 (middle), showing similar bands of cloud structure and turbulent features. White bands are often called zones and reddish bands are called belts. An Infrared Telescope Facility (IRTF) image of Jupiter at 4.85 microns (right) shows ‘hot spots’ associated with belts.

2.0 MODEL ATMOSPHERIC PROFILE

The general composition and properties of Jupiter’s atmosphere are well known since Voyager. Fig. 2a shows the profiles of key molecular constituents and temperature. Atmospheric profile data was compiled from several sources [9],[10],[11]. While molecular profiles are fairly well accepted and used with small variations by many different planetary sciences groups, cloud models are quite varied, often even for the same region. Cloud layer profiles developed for Jupiter by planetary scientists are typically specific to a particular region, usually associated with a particular measurement. Fig. 2b shows the critical values for three cloud layers and a haze layer used for comparison to measurements in belt and zone regions. Three cloud layers and a haze layer are generally used to obtain sufficient degrees of freedom to match measurements over broad spectral regions. Because the adjustment of the cloud base, top and scale height were factors in the definition of the profiles for different structures, new code was developed to allow for easier adjustment of the cloud profile in the RT model.

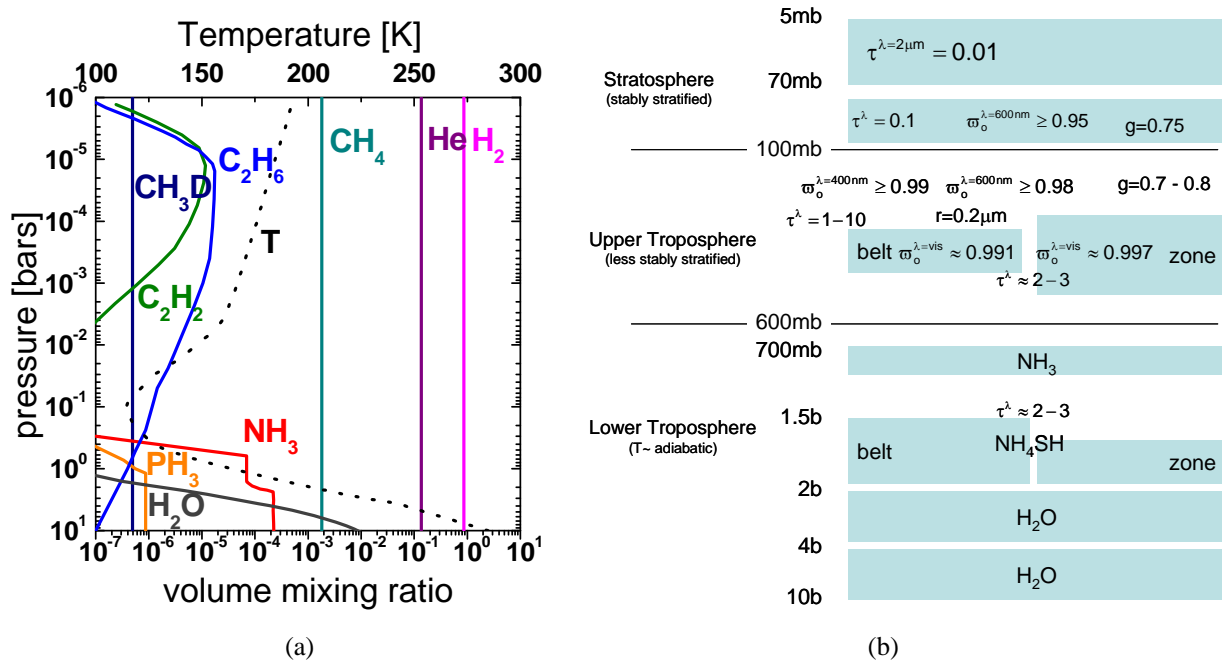


Fig. 2. Atmospheric Profiles Used in Comparison Study. a) Molecular constituents and temperature (dotted line). b) Example belt and zone cloud and haze profiles from [1].

3.0 MODEL RESULTS

Fig. 3 shows a comparison of the radiance due to molecular contributions (no clouds or haze) of Earth, Jupiter, Saturn and Neptune using the planetary RT model and profiles from Fig. 2a. The atmospheric profiles of Saturn and Neptune were described in detail in papers presented to this conference in previous years [6],[7]. Regions of solar reflection and thermal emission are shown. For Earth, with an average temperature of $\sim 300\text{K}$, the thermal emission overwhelms solar reflection around 3 microns wavelength, while for the cooler more distant planets, the crossover occurs between 3.5 and 4.5 microns. Jupiter's vertical temperature profile, measured by the Galileo probe [12] ranges between 110 and 280K over 0.001 mbar to 10 bars atmospheric pressure, while Saturn and Neptune have even lower temperatures in this pressure range. Jupiter and Saturn are closely comparable in return from reflection while Neptune exhibits similar structure but lower overall return because of its significantly greater distance from the sun. The absorption structure of the Gas Giants is dominated by CH_4 and collision induced absorption from H_2 complexes, while Earth is dominated by H_2O and CO_2 .

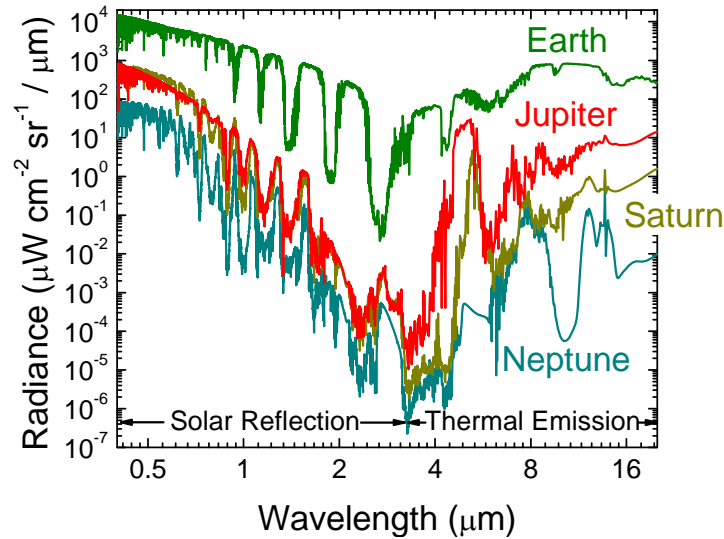


Fig. 3. Comparison of 'Clear Sky' Radiance from Earth and Gas Giants Jupiter, Saturn and Neptune.

Details of the transmission effects of molecular constituents of Jupiter are shown in Fig. 4 from 0.4 to 20 μm . The upper most plot shows details from all sources nadir from space down to three atmospheric pressure levels of 100mbars, 1 bar and 10 bars. Penetration below 10 bars is nearly impossible over much of this spectral region, with the exception of a number of residual window bands short of 1 μm ; these regions are each further obscured by particulate clouds. The second plot down from the top of Fig. 4 shows the significant role of methane, CH_4 , in the reduction of transmission, followed by ammonia, NH_3 in the third plot down. The fourth plot down shows the additional contributions of water, acetylene (C_2H_2), Ethane (C_2H_6), Phosphine (PH_3), as well as Rayleigh scatter at 10 bars. Finally, the attenuation at 1bar from collision induced absorption by dimers $\text{H}_2\text{-CH}_4$, $\text{H}_2\text{-H}_2$ and $\text{H}_2\text{-He}$ is shown in the bottom plot.

3.1 Clear Sky Model Comparisons to Data

The mid IR region, between 7 and 20 μm (1400 and 500 cm^{-1}), exhibits very low transmission for pressure layers below a few hundred mbars pressure. In this higher altitude region, a clear sky model often produces satisfactory results. Comparison is made here to the Cassini Composite Infrared Spectrometer (CIRS) instrument data [13]. The instrument collects both far-infrared (17-1000 microns) and mid-infrared (6.6-17 microns) data. In Fig. 5 we compare the planetary RT model to a CIRS spectrum averaged from measurement data between 15° S and 15° N of the equator. The spectra between 700 and 750 cm^{-1} (14.0 to 13.3 microns) are shown in Fig. 5a; the planetary RT model spectrum was generated using a 0.5 cm^{-1} FWHM resolution Gaussian slit function. Peak and value points from the data across the broader spectrum (10 to 16.7 microns), reformulated as brightness temperature, are compared in Fig. 5b.

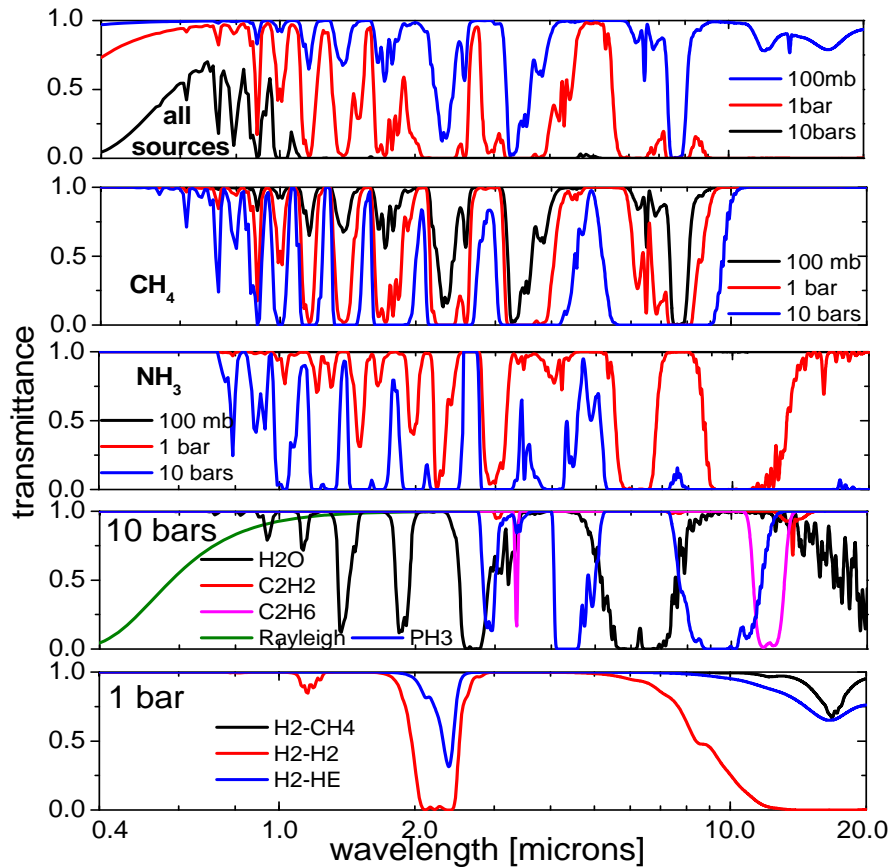


Fig. 4. Spectral Transmittance of Jupiter's Molecular Constituents. They are for vertical path from space to the indicated pressure altitude.

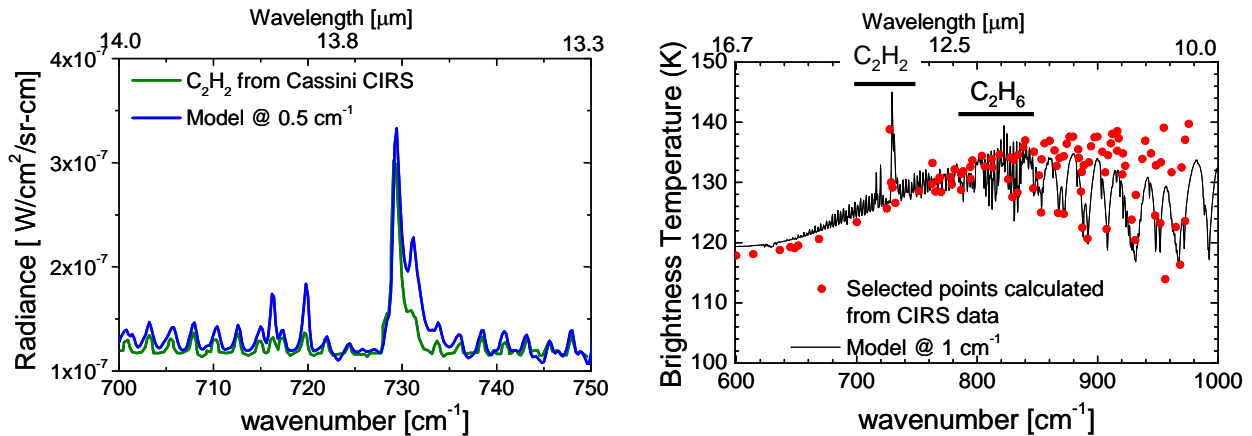


Fig. 5. Comparison to Cassini Composite Infrared Spectrometer (CIRS) data of acetylene presented in [13]. The modeled spectral radiances were convolved with a 5 cm^{-1} Gaussian slit: (a) the radiance spectra highlighting the ethylene feature and (b) the broader spectra plotted as brightness temperatures.

The sub-millimeter wave spectral region penetrates deep into the atmosphere with very little interference from clouds. Fig. 6 contains a comparison between data from 4 measurement campaigns and clear sky model calculations

by [14] with a planetary RT model calculation. The planetary RT model data were generated with a 0.5 cm^{-1} Gaussian slit filter. These calculations are strongly dependent on the input temperature profile. From $1\text{--}15 \text{ cm}^{-1}$, the brightness temperature is almost entirely dependent on the temperature profile at pressures greater than 1 bar. The planetary RT fit to the data was very sensitive to shifts in the lower boundary of the tropopause of a few bars. Both model spectra lie within the scatter of the measured data.

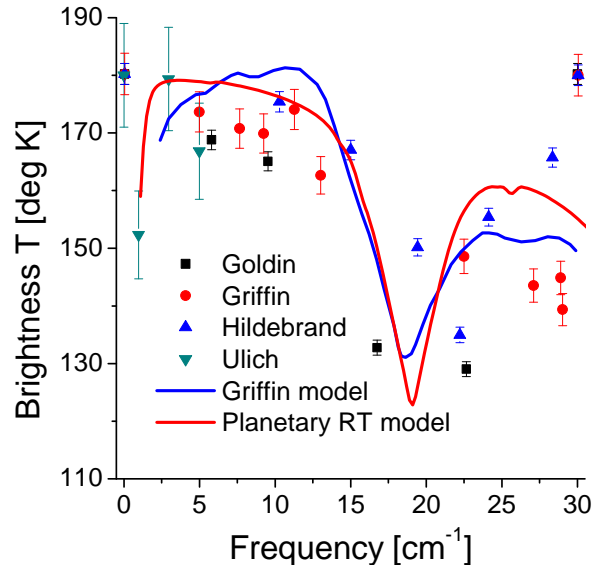


Fig. 6. Comparison of Planetary RT Model to Data from Four Measurement Campaigns and the Model of Goldin et al.[14].

3.2 Cloud Model Comparisons to Data

As observed in Fig. 4, a number of bands in the NIR spectral region, between 1.0 and $2.0 \mu\text{m}$ are transmissive down to pressures of 10 bars and the mid-IR region between 4 and 5 microns has about 50% transmission to that pressure. However the two regions have different responses to cloud opacity and molecular absorption, and therefore provide an opportunity to constrain the Jovian atmosphere specification. [15] was able to obtain excellent agreement with 4 Galileo Near-Infrared Mapping Spectrometer (NIMS) real time hot spot spectra, which they labeled RT1 (coolest) to RT4 (warmest). A comparison of the RT4 spectrum to our planetary RT calculation is shown in Fig. 7.

The fit of Fig. 7, between the planetary RT model calculation and NIMS data, is reasonably good, but 2 bite outs in the radiance at 1.5 and $1.95 \mu\text{m}$ are yet unaccounted for. These result from over prediction of NH_3 absorption. For the current effort, the NH_3 band model, which was adopted from MODTRAN[®]5 and was based on HITRAN2008 data [16], [17], was inadequate. NH_3 absorption features near $5 \mu\text{m}$ and in the near-IR and visible that are important for modeling Jupiter are either incomplete or missing from HITRAN. Recently, [8] derived temperature dependent absorption coefficient and band model data for NH_3 in the 0.74 to $5.24 \mu\text{m}$ spectral range. Initially, we attempted to defined MODTRAN[®]5 band model data between 105 and 305K based on their band model description. However, the NH_3 measurements only extended down to 215K, and extrapolation of that band model down to 105K was not successful. As an interim solution, we were able to extrapolate the absorption coefficient data to the lower temperatures. However, this data could only be integrated into the planetary RT model using a Beer's Law description, which over estimates absorption. Thus, even though we correctly include the NH_3 absorption near $5 \mu\text{m}$, there is too much absorption at 1.5 and $1.95 \mu\text{m}$. Future efforts will include development of short wave NH_3 band model data for integration into the RT model.

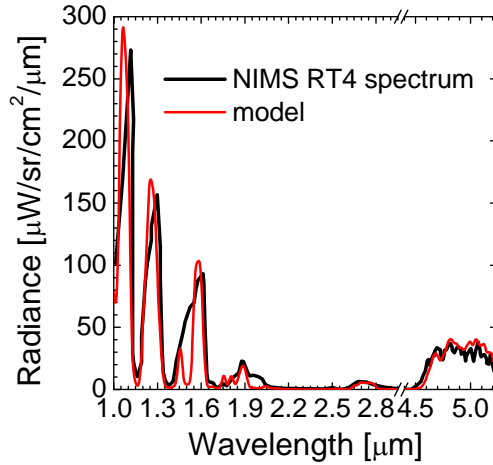


Fig. 7. Comparison of Planetary RT Model to NIMS Near-IR reflected solar and mid-IR thermal structure in a Jovian hot spot region.

The details of the cloud model for the comparison required some investigation. Optimally, we would have simply adopted the retrieved atmospheric characterizations of [15] to validate the planetary RT model. This turned out to be a difficult exercise because critical parameters were not provided in the reference. These included cloud particle to gas scale height ratios, scattering phase functions and calculation of the bottom pressure. These parameters of the model calculation were therefore based on information gleaned from other authors investigating NIMS data combined with assumptions which are described below.

While retrieved cloud base heights were reported for the 4 clouds (Lower, Middle, Upper and Haze) along with a particle to gas scale height ratio of 0.25 for the 3 upper clouds, and a 1 km thickness for the Lower cloud, The cloud tops for the 3 highest clouds were not specified. We chose to use the scale height ratio of 0.25 for all 4 clouds and set each cloud top at the pressure for which cloud density had dropped to one-quarter of the cloud base value. Spectral curves were provided for the retrieved cloud optical depth and single scattering albedo for the RT4 measurement, but these included large error limits. We adopted the retrieved optical depths, but we found we needed to use the maxima of the single scattering albedo curves for the 3 upper clouds, thus maximizing the cloud back scatter. The resultant profiles are shown in Fig. 8.

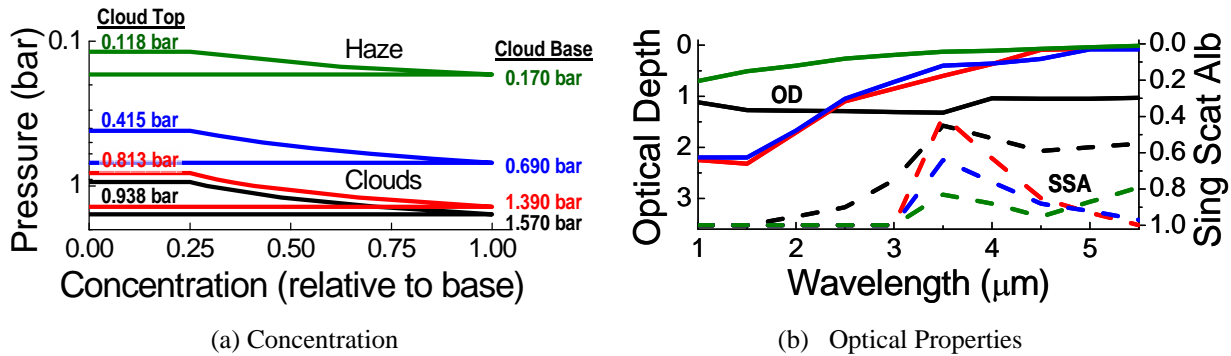


Fig. 8. Profiles of Haze and 3 Cloud Layers for the Planetary RT Model Comparison to NIMS Data. Haze (green), Upper NH₃ (blue) Middle NH₄SH (red) and Lower H₂O/NH₃/NH₄SH solution (black)

The most significant cloud unknowns were the scattering phase functions. Reference [15] indicated that initially Mie calculations were performed assuming 0.5 μm radius tholins for the haze, 0.75 μm radius NH₃ particles for the upper cloud, 0.45 μm radius NH₄SH particles for the middle cloud, and 50 μm radius NH₄SH particles for the lower cloud. The resulting phase functions were then parameterized in terms of a spectrally-independent double Henyey-Greenstein (dHG) function. These parameters were optimized as part of the fitting algorithm. The 12 parameters required to define the 4 cloud dHG functions were not provided. As a result, dHG parameters for the haze ($g = 0.75$)

and middle clouds ($f_1 = 0.938$, $g_1 = 0.8$ and $g_2 = -0.7$) were taken from Table II of [18], while the lower cloud was modeled with isotropic scattering.

Problems also arose matching the molecular absorption. Although [15] provided volume mixing ratios (VMRs) for all contributing molecules, calculation of the bottom pressure is not reported. This value dictates the gas column densities. Thus, their scattering calculation retrieved a H₂O relative humidity of $9.9 \pm 2.2\%$. Using a bottom pressure of 10 bar and a spectrally constant 0.1 bottom reflectivity (results were not sensitive to this value), we retrieved a value of 0.1% relative humidity. This is a significant discrepancy, but the water column amount is extremely sensitive to bottom pressure because of the very steep temperature increase with pressure (Fig. 2).

4.0 CONCLUSIONS

A modified version of MODTRAN@5 has been demonstrated to produce good comparison results to a variety of data and specialized RT models of Jupiter over the full electro-optical spectrum from 0.4 microns to 1 mm wavelengths. The results show the importance and complexity of cloud structure to spectroscopy of a Jupiter-like planet. This indicates that methods to insert and adjust cloud height and optical properties easily within the input profile will be of benefit. We have created a prototype of such a code for this work. The need for improved low temperature ammonia spectral band model parameters has also been identified and will be an important part of future efforts.

5.0 REFERENCES

1. <http://planetquest.jpl.nasa.gov>
2. Clampin, M., AST2010 Science Whitepaper JWST Transit Science Comparative Planetology: Transiting Exoplanet Science with JWST, 2009.
3. Seager, S. & Sasselov, D.D. Theoretical transmission spectra during extrasolar giant planet transits. *Astrophys. J* 537, L916–L921, 2000.
4. Hubbard, W.B., Fortney, J. J., Lunine, J. I., Burrows, A., Sudarsky, D., & Pinto, P. Theory of Extrasolar Giant Planet Transits, *ApJ*, 560, 413–419, 2001.
5. Berk, A., Anderson, G.P., Acharya, P.K., Bernstein, L.S., Muratov, L., Lee, J., Fox, M., Adler-Golden, S.M., Chetwynd, J.H., Hoke, M.L., Lockwood, R.B., Gardner, J.A., Cooley, T.W., Borel, C.C., Lewis, P.E., and Shettle, E.P., MODTRAN5: 2006 Update, *Proc. SPIE*, Vol. 6233, 62331F, 2006.
6. Berk, A., Bernstein, L. S., and Duff, J. W., Application of MODTRAN[®] to Planetary Atmospheres, AMOS Conf. Proc., 2008.
7. Bernstein, L. S., Berk, A., and Sundberg, R. L., Application of MODTRAN[™] to Extra-Terrestrial Planetary Atmospheres, 2007 AMOS Technology Conference, Maui, HI, 2007.
8. Bowles, N., Calcutt, S., Irwin, P., Temple, J., Band parameters for self-broadened ammonia gas in the range 0.74 to 5.24 μm to support measurements of the atmosphere of the planet Jupiter, *Icarus*, Vol. 196, 612–624 (2008).
9. Banfield, D., Gierasch, P. J., Bell, M., Ustinov, E., Ingersoll, A. P., Vasavada, A. R., West, R. A., and Belton, M. J. S., Jupiter's Cloud Structure from Galileo Imaging Data, *ICARUS* vol. 135, 230–250 (1998)
10. Nixon, C. A., Irwin, P. G. J., Calcutt, S. B., Taylor F. W., and Carlson R. W., Atmospheric Composition and Cloud Structure in Jovian 5- μm Hotspots from Analysis of Galileo NIMS Measurements *Icarus* Vol. 150, 48–68 (2001).
11. de Pater, I., DeBoer, D., Marley, M., Freedman, R., Young, R., Retrieval of water in Jupiter's deep atmosphere using microwave spectra of its brightness temperature, *ICARUS* vol. 173, 425-438 (2005).
12. Seiff, A., Kirk, D. B., Knight, T. C. D., Mihalov, J. D., Blanchard, R. C., Young, R. E., Schubert, G., von Zahn, U., Lehmacher, G., Miles, F. S., and Wang, J., Structure of the atmosphere of Jupiter: Galileo probe measurements. *Science* vol. 272, 844–845, 1996.
13. Nixon, C. A., Achterberg, R. K., Conrath, B. J., Irwin, P. G. J., Teanby, N. A., Fouchet, T., Parrish, P. D., Romani, P. N., Abbas, A., LeClair, M., Strobel, D., Simon-Miller, A. A., Jennings, D. J. Flasar, F. M. and Kunde, V.G., Meridional variations of C₂H₂ and C₂H₆ in Jupiter's atmosphere from Cassini CIRS Infrared spectra, *Icarus*, Vol. 188, 47–71 (2007).

14. Goldin, A. B., Kowitt, M. S., Cheng, E. S., Cottingham, D. A., Fixsen, D. J., Inman, C. A., Meyer, S. S., Puchalla J. L., Ruhl, J. E., and Silverberg, R. F., Whole-Disk Observations Of Jupiter, Saturn, And Mars In Millimeter/Submillimeter Bands, *The Astrophysical Journal*, vol. 488:L161–L164, 1997.
15. Irwin, P. G. J., Weir, A. L., Smith, S. E., Taylor, F. W., Lambert, A. L., Calcutt, S. B., Cameron-Smith, P. J., Carlson, R. W., Baines, K., Orton, G. S., Drossart, P., Encrenaz, T. and Roos-Serote, M., Cloud structure and atmospheric composition of Jupiter retrieved from Galileo near-infrared mapping spectrometer real-time spectra, *J. Geophys. Res.*, Vol. 103, no. E10, 23,001–23,021, 1998.
16. Rothman, L.S., *et al.*, The HITRAN 2008 molecular spectroscopic database. *J. Quant. Spectrosc. Radiat. Transfer*, Vol. 110, 533–572 (2009).
17. Rothman, L.S., <http://cfa-www.harvard.edu/hitran/>.
18. Chanover, N. J., Kuehn, D. M., and Beebe, R. F., Vertical Structure of Jupiter's Atmosphere at the Galileo Probe Entry Latitude, *ICARUS* vol. 128, 294-305, 1997.